

To appear in *Astronomy Reports*, 2016, Vol. 60, No. 5

Features of the Matter Flows in the Peculiar Cataclysmic Variable AE Aquarii

P.B. Isakova*, N.R. Ikhsanov^{†,**}, A.G. Zhilkin^{*,‡}, D.V. Bisikalo* and N.G. Beskrovnaya[†]

**Institute of Astronomy, Russian Academy of Sciences, ul. Pyatnitskaya 48, Moscow, 119017 Russia*

[†]*Central (Pulkovo) Astronomical Observatory, Russian Academy of Sciences, Pulkovskoe shosse 65, St. Petersburg, 196140 Russia*

***St. Petersburg State University, Universitetskii pr. 28, Petrodvorets, 198504 Russia*

[‡]*Chelyabinsk State University, ul. Brat'yev Kashirinykh 129, Chelyabinsk, 454001 Russia*

Abstract.

The structure of plasma flows in close binary systems in which one of the components is a rapidly rotating magnetic white dwarf is studied. The main example considered is the AE Aquarii system; the spin period of the white dwarf is about a factor of 1000 shorter than the orbital period, and the magnetic field on the white dwarf surface is of order of 50 MG. The mass transfer in this system was analyzed via numerical solution of the system of MHD equations. These computations show that the magnetic field of the white dwarf does not significantly influence the velocity field of the material in its Roche lobe in the case of laminar flow regime, so that the field does not hinder the formation of a transient disk (ring) surrounding the magnetosphere. However, the efficiency of the energy and angular momentum exchange between the white dwarf and the surrounding material increases considerably with the development of turbulent motions in the matter, resulting in its acceleration at the magnetospheric boundary and further escape from the system at a high rate. The time scales of the transition of the system between the laminar and turbulent modes are close to those of the AE Aqr transition between its quiet and active phases.

Keywords: Accretion and accretion disks, magnetic fields, Magnetohydrodynamics, binaries: close, white dwarfs, stars: individual(AE Aquarii)

PACS: 97.30.Qt, 97.10.Gz, 97.20.Rp, 97.80.-d, 83.60.Np, 95.30.Qd

INTRODUCTION

AE Aquarii is one of the most actively studied cataclysmic variables [1]. It is located at a relatively small distance ($d = 100 \pm 30$ pc) and has a binary orbital period, $P_{\text{orb}} \simeq 9.88$ hr, and a low eccentricity, $e \simeq 0.02$ [2, 3]. The binary contains a K3–K5 red dwarf and a strongly magnetized white dwarf which rotates at extremely short period, $P_{\text{spin}} \simeq 33$ s [4]. The limits for the orbital inclination are $43^\circ < i < 70^\circ$, with the most probable value of $55^\circ \pm 7^\circ$. The ratio of the masses of the red dwarf, M_d , and the white dwarf, M_a , is $q = M_d/M_a \sim 0.6\text{--}0.8$ (see [2, 5, 6] and references therein).

The bolometric luminosity of the system from the radio to the X-rays is $L_{\text{bol}} \simeq 10^{33}$ erg/s. A relatively small fraction ($10^{-6}\text{--}10^{-4}$) of this energy is emitted in the radio, where the system manifests itself as a non-thermal variable source [7]. The

radiation is predominantly thermal in other wavebands, and can be well approximated by a superposition of three spatially separated sources. The radiation of the red dwarf dominates in the infrared and optical domains (70%–95%). The contribution of the white dwarf does not exceed 2% of the bolometric luminosity of the system; the white dwarf is revealed through its regular pulsations with the period of 33 s, which are observed in the optical, ultraviolet (UV), and X-ray. The third source has a strongly variable continuum and emission lines in the optical, UV, and X-rays. This source is associated with the material which moves in the Roche lobe of the white dwarf and flows away from the binary. This source is probably responsible for the unique flaring activity of the star, which has no analogs among all known classes of non-stationary objects.

Henize [8] was the first to report the unusually rapid variations of AE Aquarii; he remarked that the flares of the star occur one after another, with a recurrence time of about an hour. Further observations have shown that the star predominantly stays in its active phase: the total duration of observations in the active state (for observations covering more than 65 years) exceeded the total duration of observations in the quiet state. Five-to-ten-minute flares are observed in the active phase, they overlap, forming series with durations from several tens of minutes to several hours. The brightness variations during flares occur synchronously in the optical, UV, and X-rays. The maximum energy release over the entire flare is in the UV, where the luminosity of the system can change by an order of magnitude over several minutes. The transition from the active to the quiet state happens without any apparent intermediate phase [9]. In the quiet state, whose duration is usually several tens of minutes, reaching two-to-three hours only in rare cases, the radiation of the system is characterized by the presence of flickering [10, 11].

The temporal structure of the flares observed in the radio is similar. However, the variations of the radio intensity do not correlate with those in other parts of the spectrum. VLBI observations of AE Aquarii show that the size of the radio source is apparently comparable to the size of the system, and that the radio emission is obviously non-thermal [12]. This suggests the action of different mechanisms generating the flares in the radio and optical, while the trigger mechanism responsible for the time characteristics of these events is probably the same for the system as a whole [13].

The most probable reason for the unique flaring activity of AE Aquarii is an unusual state of its white dwarf. The observed spindown rate of the object, $\dot{P}_0 = (5.64 \pm 0.02) \times 10^{-14}$ s/s [14, 15], implies that its spindown power,

$$L_{\text{sd}} = I\omega_s\dot{\omega}_s \simeq 6 \times 10^{33} I_{50} P_{33}^{-3} \left(\frac{\dot{P}_s}{\dot{P}_0} \right) \text{ erg} \cdot \text{s}^{-1}, \quad (1)$$

is a factor of 120–300 higher than the luminosity of the system in the UV and X-rays, and more than a factor of five higher than its bolometric luminosity, L_{bol} . Here, $\omega_s = 2\pi/P_{\text{spin}}$ is the angular velocity of the white dwarf rotation; $\dot{\omega}_s = d\omega_s/dt$; P_{33} and I_{50} are the period and the moment of inertia of the white dwarf in units of 33 s and 10^{50} g · cm², and $\dot{P}_s = dP_{\text{spin}}/dt$. This situation, with the spindown power of the star considerably exceeding its luminosity, is quite atypical for cataclysmic variables. Among all types of sources in our Galaxy, this property is characteristic only of ejecting pulsars, whose spindown power is transformed predominantly into the energy of relativistic winds and electromagnetic and MHD waves. Ikhsanov [16] was the first to draw attention to this

situation, having estimated the magnetic moment of the white dwarf using the formula for magneto-dipole losses:

$$\mu \simeq 10^{34} P_{33}^2 \left(\frac{L_{\text{sd}}}{6 \times 10^{33} \text{ erg} \cdot \text{s}^{-1}} \right)^{1/2} \text{ G} \cdot \text{cm}^3. \quad (2)$$

In this case, the mean magnetic field at the surface of the white dwarf is ~ 50 MG (see also [17]).

The basis for the first doubts about the accretion nature of the emission from AE Aquarii was provided by observations with the Hubble Space Telescope [18]. They made it possible to identify the source of the 33s (and 16.5 s) pulsations observed in the optical and UV with two diametrically opposite spots located on the surface of the white dwarf (probably in the regions of its magnetic poles). The temperature of these regions, $T_p \sim 26000$ K, exceeds the mean surface temperature of the white dwarf, $T_{\text{wd}} \sim 10000\text{--}16000$ K, by no more than a factor of three. It was also found that the intensity of the pulsating component in the optical and UV remained virtually constant during flares, ruling out explanations of the flaring activity of the system in terms of non-stationary accretion of material onto the white dwarf surface.

These doubts were made stronger by the results of X-ray observations. The X-ray spectrum, with a much lower intensity than in the UV, was found to be exceptionally soft [19, 20], resembling a coronal spectrum rather than an accretion-powered spectrum [12]. Moreover, the source of non-pulsating X-rays, whose contribution exceeds 80% in quiescence and reaches 93% during flares [21], is larger in size than the white dwarf radius by a factor of more than ten [22]. Finally, the power spectrum based on X-ray data lacks a harmonic corresponding to the 16.5-s period. The phase diagram clearly shows the contribution of one of the spots to both the X-ray and UV emission from the system, while the second spot contributes only in the UV, with the X-ray intensity reaching its minimum at this phase [21].

The final conclusion that the standard scenario with disk accretion onto the surface of the white dwarf was not able to describe the mass transfer and emission processes in the AE Aquarii system was based on an analysis of optical spectrograms, in particular, H_α Doppler tomograms. The distance from the white dwarf to the point where the material approaches it most closely exceeds the white dwarf radius by a factor of 30–70 [23, 24]. It was also noted that the H_α Doppler tomograms presented in [23, 25] showed no signs of the presence of a developed Keplerian accretion disk in the system. On the contrary, they correspond to the case when material flowing into the Roche lobe of the white dwarf through the Lagrangian point L_1 leaves the system after interacting with the magnetic field of the rapidly rotating white dwarf (see [6] and references therein).

The current model of AE Aquarii based on the observations described above is able to explain the rapid braking by the rotation of the white dwarf (in the framework of the standard model for a radio pulsar) and the presence of hot spots by the dissipation of the back current in its magnetosphere, and to identify the additional extended radiation source with material flowing in the Roche lobe of the white dwarf and leaving the system. At the same time, the origin of the flaring activity of the object remains an open question in this model. The lack of correlation of the flares with the orbital phase [10] and the high luminosity during the strongest flares (comparable to the mean bolometric

luminosity of the system [9]) make it impossible to explain the flares in terms of magnetic flaring activity of the red dwarf. It is more plausible that the source of the flares observed in the optical, UV, and X-ray is inside the Roche lobe of the white dwarf. An increase in the effective area (volume) of the extended source [9, 26] and a considerable broadening of the emission line wings [2, 5] during flares support this hypothesis. In this case, the brightness variations reflect the non-stationary character of the energy and angular momentum exchange between the white dwarf and material flowing between the system components.

Until recently, the interaction between the magnetic field of the white dwarf and the material flowing in its Roche lobe was studied using several simplifying assumptions. In particular, the stream of matter was modeled as a superposition of diamagnetic blobs, treated like test particles in the computations. Deformation and heating of the blobs were neglected. The rate of change of the kinetic energy of the blobs moving relative to the magnetic field of the white dwarf was normalized to its maximum value, and the correction coefficient was estimated empirically, by comparing the computational results to the velocity field derived from observed H_α Doppler tomograms [23, 24]. In this approach, the velocity dispersion of the material outflow was interpreted in terms of the differences in the masses and radii of the test particles, leading to differences in the trajectories of their motion in the Roche lobe of the white dwarf. The cause for fragmentation of the initial stream into plasma condensations was not considered.

The results of computations of mass transfer in low-mass binaries performed using a full set of MHD equations confirm the possibility of a scenario where a stream of matter leaves the system after interaction with the white dwarf magnetosphere [27, 28] (see also [29]). Such objects have acquired the name “super-propellers”¹ [28]. These magnetic white dwarfs rotate so rapidly that the linear velocities at their magnetosphere boundaries considerably exceed the Keplerian velocities. It was also noted that the process of interaction between a superpropeller and the material surrounding its magnetosphere is unstable, and its efficiency depends significantly on the physical parameters of matter located at the magnetospheric boundary. This provides a wide variety of possible scenarios for mass transfer in the system (from the formation of a transient disk to the complete suppression of mass exchange between the components via the Lagrangian point L_1), including periodic replacement of one flow type with another on the dynamical time scale.

In this study, we have analyzed possibilities for describing the plasma flows in AE Aquarii in the superpropeller model. In Section 2, we analyze the efficiency of the interaction between the magnetosphere of the white dwarf and the material flowing into its Roche lobe from L_1 , taking into account the conductivity of this stream. Section 3 describes the numerical model used. The results of our numerical computations of the mass transfer picture presented in Section 4 indicate possible formation of a transient disk in the system, with a typical life time up to several hours. Observable characteristics of the source within this scenario are discussed in Section 5.

¹ Note that the term “super-propeller” is sometimes used in a somewhat different sense. For example, the term “superpropeller mode” is applied to the propeller mode under the conditions of super-critical accretion in [30].

INTERACTION OF THE MAGNETIC FIELD WITH THE STREAM OF PLASMA

We consider a plasma stream flowing in the magnetic field of a rapidly rotating white dwarf. Mass transfer between the components takes place in semidetached binaries, leading to the formation of a gaseous stream which leaves the donor star envelope through the inner Lagrangian point L_1 , enters the Roche lobe of the accreting star and moves along almost a ballistic trajectory.

The interaction between the stream material and the magnetic field of the white dwarf can be fairly complex. We performed a detailed analysis of possible physical mechanisms which could contribute to changing the efficiency of the transfer of additional angular momentum from the rotating magnetosphere to the material. In particular, we considered [31] the partial ionization of plasma in the stream, the pressure of magnetodipole radiation or a relativistic stellar wind from the rotating white dwarf, the relativistic retard of the magnetic field lines, and incomplete penetration of the magnetic field into plasma. We have concluded that the latter effect probably plays the most important role in the case of AE Aquarii system. It is accordingly this effect that we considered in our numerical modeling and used to explain the observational manifestations of processes in AE Aquarii.

Let us briefly elucidate the essence of this effect. The plasma stream has a diamagnetic effect. This diamagnetism is related to the following known property of plasma (see, for instance, [32, 33]). When a clump of plasma enters an external magnetic field, currents are generated on its surface, creating their own magnetic field. The current generation in this case is such that the magnetic field induced in the plasma clump cancels out the external magnetic field almost completely (apart from a thin surface layer). The external field penetrates gradually, due to diffusion processes.

Initially, only the magnetic field which was present in the secondary envelope is present in the stream. This field is determined by the magnetic field of the white dwarf which has penetrated into this region, as well as by the intrinsic magnetic field of the donor star [34]. Due to freezing of the field into the plasma, this magnetic field is transported into the Roche lobe together with the stream of plasma. However, this magnetic field is much weaker than the magnetic field in the white dwarf magnetosphere.

Let us calculate the force of the interaction between the plasma stream and the external magnetic field. When a conducting body moves in a rarefied magnetized plasma, electric fields and currents are induced on the surface of the body. This results in electromagnetic braking of the body, and the generation of Alfvén and magnetosonic waves. This type of interaction of conducting bodies during their motion in a rarefied magnetized plasma is called an induction interaction [35, 36, 37].

We can apply these considerations to our case. Under our assumptions, the total force acting on the stream is

$$\mathbf{F}_* = \frac{1}{c} \int_{\delta V} (\mathbf{j} \times \mathbf{B}) dV, \quad (3)$$

where c is the speed of light, and \mathbf{j} is the induced current density in a surface layer of the stream occupying a volume δV . The current density is determined by the induced

magnetic field arising due to the motion of the gas stream in the external field:

$$\mathbf{j} = \hat{\sigma} \cdot \mathbf{E}, \quad \mathbf{E} = \frac{1}{c} (\mathbf{u} \times \mathbf{B}), \quad (4)$$

where $\hat{\sigma}$ is the conductivity tensor of the stream material. For simplicity, we neglected magnetization and assumed that the conductivity could be described with a constant scalar coefficient σ (as in MHD). Substituting expressions (4) into (3), we obtain the estimate

$$\mathbf{F}_* = -\frac{\sigma}{c^2} \delta V B^2 \mathbf{u}_\perp, \quad (5)$$

where \mathbf{u}_\perp is the component of the velocity \mathbf{u} perpendicular to the magnetic field lines. The corresponding specific force is

$$\mathbf{f}_* = -\frac{\sigma B^2}{c^2 \rho} \frac{\delta V}{V} \mathbf{u}_\perp, \quad (6)$$

where ρ is the density of the material in the stream.

We denote the diffusion coefficient of the magnetic field in the stream plasma as $\eta = c^2/(4\pi\sigma)$. Then, we obtain the final expressions in the form

$$\mathbf{f}_* = -\frac{\mathbf{u}_\perp}{t_w}, \quad t_w = \frac{4\pi\rho\eta}{B^2} \frac{V}{\delta V}. \quad (7)$$

Note that, compared to the formula for the relaxation time t_w used in our earlier computations (e.g., [27, 28]), Eq. (7) contains an additional coefficient, $V/\delta V$, due to the presence of a diffusion layer. In the case of complete penetration of the magnetic field into the stream plasma, when the volume of the diffusion layer δV coincides with the volume of part of the stream V , Eq. (7) for the relaxation time becomes simpler, and acquires the form

$$t_w = \frac{4\pi\rho\eta}{B^2}. \quad (8)$$

In the opposite limiting case, when the diffusion layer depth is $\delta \ll R$ (where R is the scale size of a plasma clump), the volume ratio is $\delta V/V = \kappa\delta/R$, so that

$$t_w = \frac{4\pi\rho\eta}{B^2} \frac{R}{\kappa\delta}. \quad (9)$$

The coefficient κ is determined by the stream geometry. For example, $\kappa = 3$ for a spherically symmetric plasma clump.

Similar expressions for the interaction force between the gas stream and the external magnetic field can be obtained using the formalism of wave MHD turbulence. This approach can apparently be applied in the case of a very strong external magnetic field [27]. The reason is that the plasma dynamics in a strong external magnetic field is characterized by a relatively slow mean motion of the particles along the magnetic field lines, a drift across the field lines, and the propagation of Alfvén and magnetosonic waves with velocities which are very high compared to their background. The structure

of such a flow can be described using an averaged representation, considering the influence of the rapid pulsation by analogy to the wave MHD turbulence. To describe the slow proper motion of the plasma, it is necessary to isolate the rapidly propagating fluctuations and apply some averaging procedure to the ensemble of wave pulsations. We will derive the main expressions, following [28], taking into account necessary corrections.

Consider the expression

$$\mathbf{E} + \frac{1}{c}(\mathbf{v} \times \mathbf{B}) = \frac{\mathbf{j}}{\sigma}, \quad (10)$$

which describes the Ohm's law for plasma in the MHD approximation [38]. Here, $\mathbf{B} = \mathbf{B}_* + \mathbf{b}$ is the total magnetic field induction, which is the sum of the unperturbed external magnetic field, \mathbf{B}_* , and the intrinsic field of the plasma, \mathbf{b} . We emphasize that Eq. (10) should be used only in the diffusion layer into which the external magnetic field penetrates. No induction currents appear in the remaining volume of the stream.

Let us write all dynamical quantities as sums of their mean values and fluctuations, for example, $\mathbf{b} = \langle \mathbf{b} \rangle + \delta \mathbf{b}$. Averaging (10), we find

$$c\langle \mathbf{E} \rangle + \langle \mathbf{v} \rangle \times \langle \mathbf{b} \rangle + \langle \mathbf{v} \rangle \times \mathbf{B}_* + \langle \delta \mathbf{v} \times \delta \mathbf{b} \rangle = \frac{c}{\sigma} \langle \mathbf{j} \rangle. \quad (11)$$

The last term on the left-hand side can be estimated using the following equation, often used in dynamo theory (e.g., [39, 40]):

$$\langle \delta \mathbf{v} \times \delta \mathbf{b} \rangle = \alpha \langle \mathbf{b} \rangle - \eta_w \text{rot} \langle \mathbf{b} \rangle, \quad (12)$$

where α is determined by the mean helicity of the flow, and η_w is the diffusion coefficient for the diffusion of the mean magnetic field due to wave MHD turbulence. We can neglect the first term (the α effect) because it describes the relatively weak and slow generation of the mean magnetic field in the accretion disk.

Averaging the Maxwell's equation,

$$\text{rot} \mathbf{B} = \frac{4\pi}{c} \mathbf{j}, \quad (13)$$

we find

$$\langle \mathbf{j} \rangle = \frac{c}{4\pi} \text{rot} \langle \mathbf{b} \rangle. \quad (14)$$

Substituting (12) and (14) into (11) yields

$$c\langle \mathbf{E} \rangle + \langle \mathbf{v} \rangle \times \langle \mathbf{b} \rangle + \langle \mathbf{v} \rangle \times \mathbf{B}_* - \eta_w \text{rot} \langle \mathbf{b} \rangle = \eta_{\text{OD}} \text{rot} \langle \mathbf{b} \rangle, \quad (15)$$

where $\eta_{\text{OD}} = c^2/(4\pi\sigma)$ is the ohmic diffusion coefficient of the magnetic field. Since, as a rule, $\eta_w \gg \eta_{\text{OD}}$, we can neglect the right-hand side. Moreover, in the case of a strong magnetic field, we can neglect the second term (compared to the third).

Then, averaging the Maxwell's equation describing the law of electromagnetic induction,

$$\text{rot} \mathbf{E} = -\frac{1}{c} \frac{\partial \mathbf{B}}{\partial t}, \quad (16)$$

we find

$$c \operatorname{rot} \langle \mathbf{E} \rangle = -\frac{\partial \langle \mathbf{b} \rangle}{\partial t} - \operatorname{rot} (\mathbf{v}_* \times \mathbf{B}_*), \quad (17)$$

where \mathbf{v}_* is the velocity of the magnetic field lines. The first term on the right-hand side of this equation is due to variations of the mean magnetic field, $\langle \mathbf{b} \rangle$, on the dynamical time scale. This term corresponds to the second term in (15) to order of magnitude. Thus, the mean electric field strength can be estimated from the expression

$$c \langle \mathbf{E} \rangle = -\mathbf{v}_* \times \mathbf{B}_*. \quad (18)$$

Leaving the dominating terms in (15), we arrive at the relation

$$\eta_w \operatorname{rot} \langle \mathbf{b} \rangle = \mathbf{u} \times \mathbf{B}_*, \quad (19)$$

where $\mathbf{u} = \langle \mathbf{v} \rangle - \mathbf{v}_*$ is the relative velocity of the stream and magnetic field lines.

The obtained expression can be used to calculate the average electromagnetic force in the equation of motion. Neglecting density fluctuations, wave magnetic pressure, and tension, we find for the full electromagnetic force acting on the gas stream

$$\mathbf{F}_{\text{em}} = -\frac{1}{4\pi} \int_V \langle \mathbf{B} \times \operatorname{rot} \mathbf{B} \rangle dV = -\frac{1}{4\pi} \int_V \langle \mathbf{b} \rangle \times \operatorname{rot} \langle \mathbf{b} \rangle dV - \frac{1}{4\pi} \int_{\delta V} \mathbf{B}_* \times \operatorname{rot} \langle \mathbf{b} \rangle dV. \quad (20)$$

The first term on the right-hand side describes the electromagnetic force due to the intrinsic magnetic field of the plasma, $\langle \mathbf{b} \rangle$. The second term, describing the force from the external field, takes into account the fact that the field \mathbf{B}_* penetrates the plasma only in the diffusion layer. We calculated this term using (19). We have

$$\mathbf{B}_* \times \operatorname{rot} \langle \mathbf{b} \rangle = \frac{B_*^2}{\eta_w} \mathbf{u}_\perp, \quad (21)$$

where the subscript \perp denotes velocity components perpendicular to the magnetic field \mathbf{B}_* .

We have obtained the following expression for the corresponding specific force:

$$\mathbf{f}_* = -\frac{\mathbf{u}_\perp}{t_w}, \quad t_w = \frac{4\pi\rho\eta_w}{B^2} \frac{V}{\delta V}. \quad (22)$$

In contrast to (7), the meaning of the diffusion coefficient is different here. However, if we do not go into the nature of the diffusion of the magnetic field, these formulae appear equivalent. Moreover, all the above calculations can be considered a modified derivation of the expression for the force \mathbf{f}_* in (7) in the framework of the induction mechanism, taking into account the effects of the wave MHD turbulence which appears in the case of a very strong external field.

DESCRIPTION OF THE MODEL

We describe the flow structure in a close binary system using a non-inertial reference frame rotating with the orbital angular velocity $\Omega = 2\pi/P_{\text{orb}}$ relative to its center of mass. In this reference frame, we choose a Cartesian coordinate system (x, y, z) , with its origin coincident with the center of the degenerate component, $\mathbf{r}_a = 0$. The center of mass of the donor star is located at the distance A from the origin along the x axis, $\mathbf{r}_d = (-A, 0, 0)$. The z axis is along the rotation axis of the system, $\mathbf{\Omega} = (0, 0, \Omega)$. In this reference frame, the rotation of the white dwarf is described by the angular velocity vector $\mathbf{\Omega}_a$. In our model, we consider the case when the rotation axis of the white dwarf coincides with the binary rotation axis. Therefore²,

$$\mathbf{\Omega}_a = \left(\frac{P_{\text{orb}}}{P_{\text{spin}}} - 1 \right) \mathbf{\Omega}, \quad (23)$$

giving $\mathbf{\Omega}_a = 1091.5\mathbf{\Omega}$ for the AE Aquarii system.

We assume that the magnetic field of the white dwarf, \mathbf{B}_* , is dipolar, and is described by the dipole moment vector $\boldsymbol{\mu}$. In the chosen coordinates, $\boldsymbol{\mu}$ has the components $\mu_x = \mu \sin \theta \cos \phi$, $\mu_y = \mu \sin \theta \sin \phi$, $\mu_z = \mu \cos \theta$, where μ is the magnitude of the vector $\boldsymbol{\mu}$, θ is the inclination of $\boldsymbol{\mu}$ to the z axis, and ϕ is the angle between the x axis and the projection of $\boldsymbol{\mu}$ onto the xy plane. Taking into account the rotation of the white dwarf, the angle ϕ is time-dependent, so that the magnetic field \mathbf{B}_* is not stationary. In the approximation of a quasi-stationary electromagnetic field, we can write: $\phi = \Omega_a t + \phi_0$, where ϕ_0 is the initial value of this angle. Note that, in a quasi-stationary approximation, the magnetic field, \mathbf{B}_* , is a potential field, $\text{rot } \mathbf{B}_* = 0$. This enables us to partially exclude it from the equations describing the structure of the MHD flows in the close binary system.

Taking into account the influence of the magnetic field, the flows of matter in the close binary system can be described using the following system of equations [28]:

$$\frac{\partial \rho}{\partial t} + \nabla \cdot (\rho \mathbf{v}) = 0, \quad (24)$$

$$\frac{\partial \mathbf{v}}{\partial t} + (\mathbf{v} \cdot \nabla) \mathbf{v} = -\frac{\nabla P}{\rho} - \frac{\mathbf{b} \times \text{rot } \mathbf{b}}{4\pi\rho} - \nabla \Phi + 2(\mathbf{v} \times \mathbf{\Omega}) - \frac{(\mathbf{v} - \mathbf{v}_*)_{\perp}}{t_w}, \quad (25)$$

$$\frac{\partial \mathbf{b}}{\partial t} = \text{rot} [\mathbf{v} \times \mathbf{b} + (\mathbf{v} - \mathbf{v}_*) \times \mathbf{B}_* - \eta \text{rot } \mathbf{b}], \quad (26)$$

$$\rho T \left[\frac{\partial s}{\partial t} + (\mathbf{v} \cdot \nabla) s \right] = n^2 (\Gamma - \Lambda) + \frac{\eta}{4\pi} (\text{rot } \mathbf{b})^2. \quad (27)$$

Here, ρ is the density in the stream, \mathbf{v} is its velocity, P is the pressure, s is the entropy per unit mass, $n = \rho/m_p$ is the number density, m_p is the proton mass, and η is the

² $P_{\text{beat}} = 2\pi/\Omega_a$ is the beat period between the rotation period of the white dwarf, P_{spin} , and the orbital period of the binary, P_{orb} . Because of the very rapid rotation of the white dwarf in the AE Aquarii system, the beat period is $P_{\text{beat}} \approx P_{\text{spin}}$.

coefficient of magnetic viscosity. The equation for the entropy (27) takes into account radiative heating and cooling, as well as heating of material due to current dissipation. The dependencies of the radiative heating function Γ and the cooling function Λ on the temperature T have fairly complex forms [41, 42, 43, 44]. Therefore, in our numerical model, we used linear approximations for these functions in the vicinity of the equilibrium temperature, 8 782 K [29, 45, 46, 47], which corresponds to the effective temperatures of all three sources of thermal radiation in the AE Aquarii system. The term $2(\mathbf{v} \times \boldsymbol{\Omega})$ in the equation of motion (25) describes the Coriolis force. The density, entropy, and pressure are related through the ideal gas law: $s = c_V \ln(P/\rho^\gamma)$, where c_V is the specific heat capacity of the gas at constant volume, and the adiabatic index is $\gamma = 5/3$.

The numerical model takes into account the effects of magnetic field diffusion [see (26)] due to magnetic reconnection and current dissipation in turbulent vortexes [48], magnetic buoyancy [49], and wave MHD turbulence [27]. The first two effects play important role in the accretion disks of intermediate polars. The third effect dominates in the region of the magnetosphere and in the accretion streams of polars. The total magnetic viscosity coefficient η , determined by all these effects, depends on the magnetic field in the plasma, \mathbf{b} . Thus, in general, the character of the magnetic field diffusion is non-linear.

The last term in the equation of motion (25) describes the force exerted by the magnetic field of the white dwarf on the plasma. This force determines the variations of the plasma velocity perpendicular to the magnetic field, \mathbf{v}_\perp . The vector

$$\mathbf{v}_* = \boldsymbol{\Omega}_a \times (\mathbf{r} - \mathbf{r}_a) \quad (28)$$

describes the velocity of the magnetic field lines of the white dwarf. The decay time scale for the transverse velocity t_w is determined by wave dissipation of the magnetic field in the diffusion layer.

We applied the 3D parallel numerical code [27, 29, 46, 47] in our MHD numerical simulation. This code is based on the Godunov-type difference scheme with the high order of accuracy. The computations used a geometrically adaptive grid [47], which concentrated towards the equatorial plane and the surface of the white dwarf. This made it possible to considerably improve the resolution of vertical structures in the accretion stream and in the region of the white dwarf magnetosphere.

DISCUSSION

We have adopted the following model parameters for the close binary system AE Aquarii [6]. The donor star (a red dwarf) has the mass $M_d = 0.91M_\odot$ and the effective temperature of 4 000 K. The mass of the white dwarf is $M_a = 1.2M_\odot$, and its effective temperature is about 13 000 K. The component separation is $A = 3.02R_\odot$. We assumed a magnetic field on the surface of the white dwarf $B_a = 50$ MG.

We have used the following boundary conditions in our computations. At the inner Lagrangian point L_1 , we take the gas velocity to be equal to the local sound speed, $c_s = 7.4$ km/s, corresponding to the effective temperature of the donor star of 4 000 K. The gas density is $\rho(L_1) = 4.7 \times 10^{-8}$ g/cm³, corresponding to the mass exchange

rate $\dot{M} = 10^{-9} M_{\odot}/\text{year}$. We have imposed constant boundary conditions at the other boundaries of the computation region. We obtained solutions in the region $(-0.53A \leq x \leq 0.53A, -0.53A \leq y \leq 0.53A, -0.26A \leq z \leq 0.26A)$, on a grid of $128 \times 128 \times 64$ cells.

To describe the flaring activity, we have analyzed the situation when the flow of plasma in the Roche lobe of the white dwarf occurs successively in two modes: laminar and turbulent. In the laminar mode, the depth of the boundary layer in the region where material interacts with the magnetic field of the white dwarf is determined by microscopic processes, and turns out to be relatively small. Under these conditions, the influence of the magnetic field on the stream is relatively weak, and the parameters of its motion do not differ strongly from those computed in a gas-dynamical approximation. In the turbulent mode, the depth of the diffusion layer sharply increases. In this case, the magnetic field penetrates deeply into the plasma of the stream and has a significant influence on its motion.

In the laminar mode, the stream bends around the magnetosphere of the white dwarf and forms a transient disk (ring). The transition of the disk to the turbulent mode occurs during its interaction with the stream arriving from the donor or/and the development of a (Kelvin–Helmholtz type) instability at the inner boundary of the disk. In the turbulent mode, the material of the transient disk quickly mixes with the magnetic field of the white dwarf, and is accelerated in the tangential direction and ejected from the Roche lobe. Further, the flow of matter which continues to arrive from L_1 returns to the laminar mode.

It is difficult to estimate the instantaneous depth of the diffusion layer in the numerical model we used. Instead, we assumed a corresponding magnetic viscosity coefficient based on some phenomenological considerations. This approach seems quite acceptable for the purposes of this study.

We have modeled the structure of the plasma flow in the Roche lobe of the white dwarf, taking into account transitions between the laminar and turbulent modes, using the numerical model described above, where the depth of the diffusion layer is expressed as

$$\frac{\delta V}{V} = 1 - \left(1 - e^{-kr}\right) f(t). \quad (29)$$

Here r is the distance from the rotation axis to a given point and k is a coefficient determining the characteristic size of the white dwarf magnetosphere. The coefficient used in our computations was $k \approx 33/A$. The function $f(t)$, displayed in Fig. 1, is periodic, with the period $P_{\text{orb}}/2$. In the initial phases of the orbital period ($0 \leq t \leq 0.3P_{\text{orb}}$), this function is equal to unity. In this case, the depth of the diffusion layer (29) is virtually zero, with the exception of the magnetosphere region close to the white dwarf. The plasma flow in the Roche lobe is laminar at this stage. At later phases of the orbital period ($0.3P_{\text{orb}} \leq t \leq 0.5P_{\text{orb}}$), $f(t) = 0$. In this case, the depth of the diffusion layer (29) is the largest ($\delta V/V = 1$), with the result that the plasma flow in the Roche lobe switches to the turbulent mode.

The results of our numerical modeling of the AE Aquarii system in the proposed scenario are presented in Figs. 2–4. The gray scale represents the distribution of the logarithm of the density in units of the density at the inner Lagrangian point, $\rho(L_1) = 4.7 \times 10^{-8} \text{ g/cm}^3$, corresponding to the mass transfer rate $\dot{M} = 10^{-9} M_{\odot}/\text{year}$. The arrows show the velocity distribution. The dotted curve corresponds to the boundary of

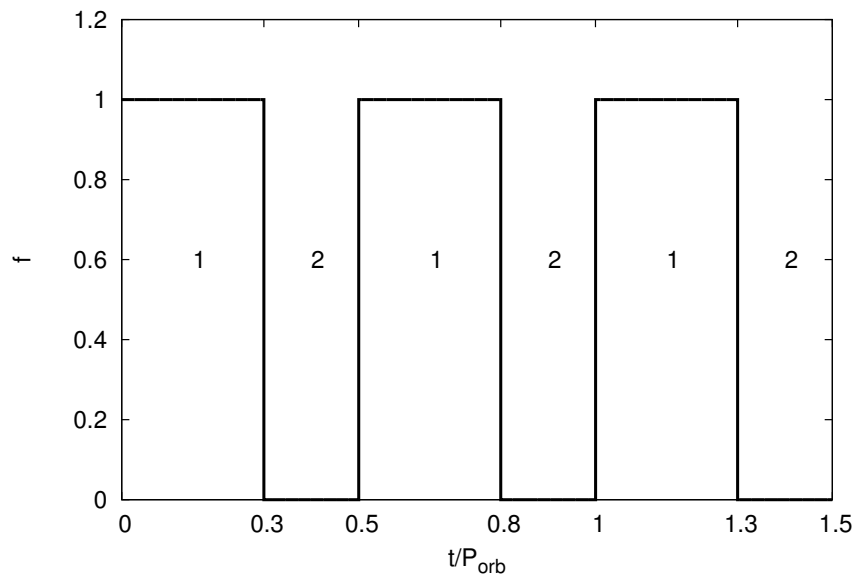


FIGURE 1. The function $f(t)$. 1 is the laminar phase, and 2 is the turbulent phase.

the Roche lobe. The white dwarf is shown as an open circle. In all these figures, the left panel corresponds to the equatorial (xy) plane of the binary and the right panel to the vertical (xz) plane.

In the quiescent phase (Fig. 2), the flow in the system is laminar. The diffusion layer is thin in this case, and the magnetic field of the white dwarf penetrates into the stream plasma only insignificantly. At the same time, however, hot, rarefied plasma rotating with the magnetic field lines can be present in the magnetosphere region. This forms a kind of corona around the rapidly rotating white dwarf, and makes it more difficult for material to penetrate this zone. In other regions, the magnetic field of the white dwarf has virtually no influence on the plasma flow. We call this the stationary laminar phase.

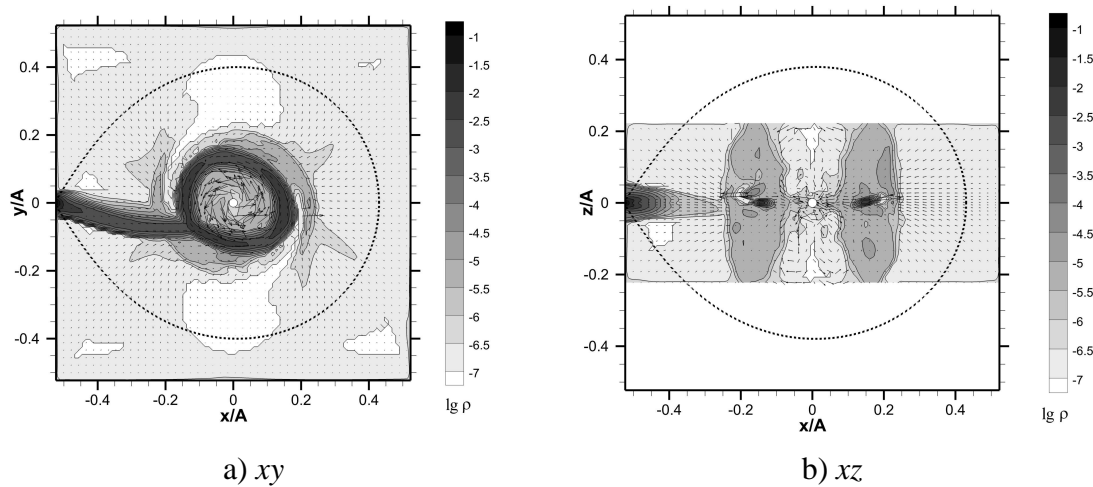


FIGURE 2. The stationary laminar phase. The density and velocity distributions in the equatorial (left) and vertical (right) planes of the binary system.

At this stage, the system forms a transient disk with a typical radius of $0.1A-0.2A$ (left panel of Fig. 2). The inner disk radius is determined by the equilibrium condition at the boundary of the white dwarf magnetosphere. The vertical structure of the flow is displayed in the right panel of Fig. 2. The white dwarf magnetosphere has the shape of a cylinder with fairly broad and relatively dense walls. The transient disk is located in the region of these walls, in the equatorial plane of the binary.

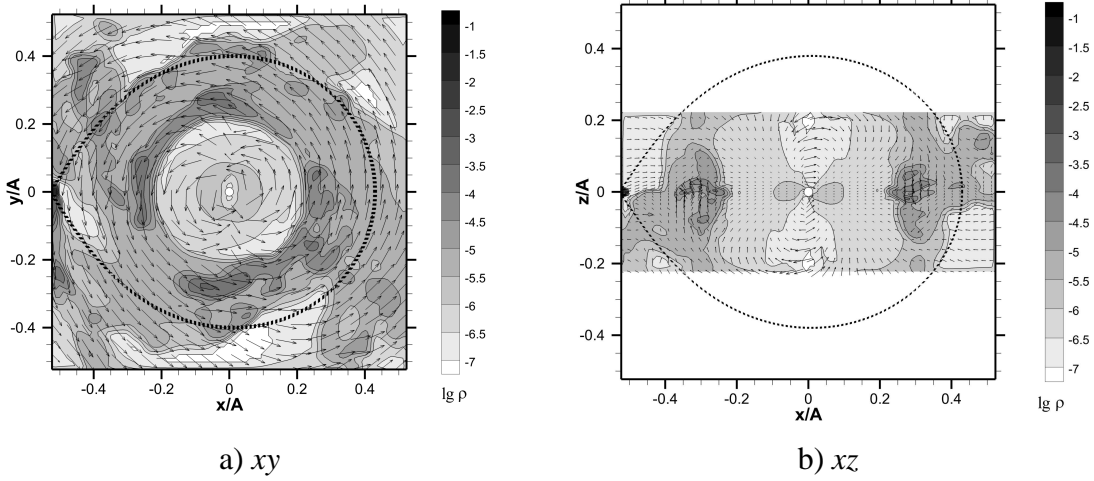


FIGURE 3. The transition phase. The density and velocity distributions in the equatorial (left) and vertical (right) planes of the binary system.

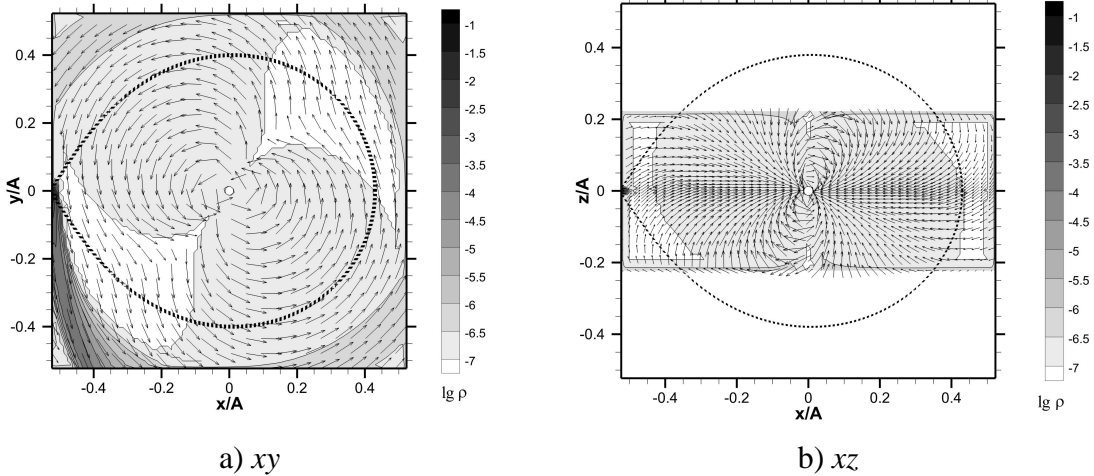


FIGURE 4. The stationary turbulent phase. The density and velocity distributions in the equatorial (left) and vertical (right) planes of the binary system.

After the end of the laminar phase, which lasts for $0.3P_{\text{orb}} \approx 3$ hrs in our model, the numerical code switches to the computational regime of the turbulent motion. The magnetic field diffusion coefficient increases rapidly in the turbulent flow compared to the laminar flow, by several orders of magnitude. The depth of the diffusion layer, where

the plasma is frozen in the magnetic field of the stream, increases considerably. The boundary of the turbulence region propagates in the material with a velocity of order of the velocity of magnetosonic waves. Thus, the entire flow region becomes turbulent on a time scale shorter than the dynamical time scale. For some time, material frozen in the magnetic field rotates rigidly, following the magnetic field lines. The initial ring is spread into a disk, and material is gradually carried beyond the limits of the Roche lobe (see Fig. 3). This flow regime can be considered a transition phase. At this time, the surface area of the disk increases, increasing its luminosity that is observationally manifested as a flare. The area of the expanding disk in Fig. 3 is approximately a factor of five to seven larger than the area of the transient disk in Fig. 2. Note that the increase in the magnetic viscosity in the transition to the turbulent mode should lead to an increase in current dissipation, and thus to a temperature increase. This is an additional factor increasing the luminosity. Thus, it is not difficult in our model to obtain a luminosity of the system which is an order of magnitude higher during the active phase than during the quiescence. This is precisely the rise of luminosity which is observed during the active phase of AE Aquarii.

The rate of material outflow beyond the limits of the system corresponds to the dynamical time scale at the boundary of the Roche lobe of the white dwarf. Matter arriving to the Roche lobe of the white dwarf through L_1 also leaves the system during this phase, interacting with the material outflow and the magnetic field of the white dwarf (see Fig. 4). This flow mode can be considered a stationary turbulent phase, and corresponds to the usual super-propeller state [28]. The duration of this stage was taken to be $0.2P_{\text{orb}}$ in our model. During all this time, the luminosity of the system decreases due to the decreasing radiation flux from the shell ejected beyond the Roche lobe. Our earlier computations of such flows show that the material outflow from L_1 forms a long trail which winds around the binary in a spiral pattern, forming a common envelope. Similar results for AE Aquarii were also obtained in other studies using the Smoothed Particle Hydrodynamics (SPH) method [23, 24].

CONCLUSIONS

The results of our computations show a wide variety of possible flow regimes in the Roche lobe of the rapidly rotating magnetic white dwarf in AE Aquarii. The flow pattern depends critically on the physical conditions in the material interacting with the magnetic field, and can change from a transient Keplerian disk (ring) to an intense, quasi-radial flow leaving the binary. Switching between the flow modes occurs on the dynamical (free-fall) time scale, which in AE Aquarii ranges from several hundred seconds, in the region where material approaches the white dwarf most closely, to several thousand seconds, in the region of L_1 . This corresponds to the characteristic time scale of the flaring activity of the system. The duration of short flares, several minutes, corresponds to the plasma turbulization time at the inner radius of the transient disk. This results in plasma heating and acceleration, with subsequent outflow from the system. The process of forming a new transient disk takes about an hour. During this time, the system is in quiescence.

The stationary flow of the stream through the Roche lobe of the white dwarf, without the formation of a Keplerian disk, discussed earlier in [23, 24], is one particular solution of the problem we have analyzed. This solution corresponds to the case of a turbulent stream whose interaction with the magnetic field of the white dwarf is close to maximally efficient. However, the question about the mechanism leading to the turbulization of the stream in such a flow pattern remains open. There are no collisions between clumps with different masses in the course of their motion in the Roche lobe of the white dwarf [24]. On the other hand, the magnetic field at the boundary of this Roche lobe is relatively weak for the parameters of interest for us, and it does not significantly influence the flow structure or its inner conditions. Finally, the relaxation time scale for turbulent motions in the stream associated with Landau damping does not exceed the dynamical time at the boundary of the Roche lobe of the white dwarf. Therefore, the stream moving along a ballistic trajectory in the Roche lobe of the white dwarf has enough time for the transition to the laminar flow regime. This implies that the outflow of matter from the system can only take place in the case of repeated turbulization of the stream in the region of its strongest interaction with the magnetic field of the white dwarf, which is confirmed by the results of our computations.

ACKNOWLEDGMENTS

P.B.I., A.G.Z. and D.V.B. were supported by the Russian Science Foundation (project 15-12-30038). N.R.I. and N.G.B. were supported by the Russian Foundation for Basic Research (project 13-02-00077).

REFERENCES

1. B. Warner, *Cataclysmic Variable Stars* (Cambridge: Cambridge Univ. Press 2003).
2. W.F. Welsh, K. Horne, and R. Gomer, *Monthly. Not. Roy. Astron. Soc.* **275**, 649 (1995).
3. M. Friedjung, *New Astron.* **2**, 319 (1997).
4. J. Patterson, *Astrophys. J.* **234**, 978 (1979).
5. K. Reinsch and K. Beuermann, *Astron. and Astrophys.* **282**, 493 (1994).
6. N. R. Ikhsanov and N. G. Beskrovnaya, *Astron. Rep.* **56**, 589 (2012).
7. T.S. Bastian, G.A. Dulk, and G. Chanmugam, *Astrophys. J.* **324**, 431 (1988).
8. K.G. Henize, *Astrophys. J.* **54**, 89 (1949).
9. N.G. Beskrovnaya, N.R. Ikhsanov, A. Bruch, and N.M. Shakhovskoy, *Astron. Astrophys.* **307**, 840 (1996).
10. A. Bruch, *Astron. Astrophys.* **251**, 59 (1991).
11. M. Eracleous and K. Horne, *Astrophys. J.* **471**, 427 (1996).
12. O.C. de Jager, *Astrophys. J. Suppl. Ser.* **90**, 775 (1994).
13. M. Abada-Simon, J. Casares, A. Evans, S. Eyres, R. Fender, S. Garrington, O. de Jager, N. Kuno, I.G. Martinez-Pais, D. de Martino, H. Matsuo, M. Mouchet, G. Pooley, G. Ramsay, A. Salama, and B. Schulz, *Astron. Astrophys.* **433**, 1063 (2005).
14. O.C. de Jager, P.J. Meintjes, D. O'Donoghue, and E.L. Robinson, *Monthly. Not. Roy. Astron. Soc.* **267**, 577 (1994).
15. W.F. Welsh, *Proc. Annapolis Workshop on Magnetic Cataclysmic Variables*, eds. C. Hellier and K. Mukai, *ASP Conference Series* **157**, 357 (1999).
16. N.R. Ikhsanov, *Astron. Astrophys.* **338**, 521 (1998).

17. N.R. Ikhsanov and P.L. Biermann, *Astron. Astrophys.* **445**, 305 (2006).
18. M. Eracleous, K. Horne, E.L. Robinson, E.H. Zhang, T.R. Marsh, and J.H. Wood, *Astrophys. J.* **433**, 313 (1994).
19. J.P. Osborne, K.L. Clayton, D. O'Donoghue, M. Eracleous, K. Horne, and A. Kanaan, in *Proc. Magnetic Cataclysmic Variables*, Eds. D. Buckley and B. Warner, ASP Conference Series **85**, 368 (1995).
20. C.-S. Choi, T. Dotani, and P.C. Agrawal, *Astrophys. J.* **525**, 399 (1999).
21. C.-S. Choi and T. Dotani, *Astrophys. J.* **646**, 1149 (2006).
22. K. Itoh, S. Okada, M. Ishida, and H. Kunieda, *Astrophys. J.* **639**, 397 (2006).
23. G.A. Wynn, A.R. King, and K. Horne, *Monthly Notices Roy. Astron. Soc.* **286**, 436 (1997).
24. N.R. Ikhsanov, V.V. Neustroev, and N.G. Beskrovnaya, *Astron. and Astrophys.* **421**, 1131 (2004).
25. W.F. Welsh, K. Horne, and R. Gomer, *Monthly. Not. Roy. Astron. Soc.* **298**, 285 (1998).
26. D. de Martino, W. Wamsteker, and G. Bromage, in *Proc. Magnetic Cataclysmic Variables*, Eds. D. Buckley and B. Warner, ASP Conference Series **85**, 388 (1995).
27. A. G. Zhilkin and D. V. Bisikalo, *Astron. Rep.* **54**, 1063 (2010).
28. A. G. Zhilkin, D. V. Bisikalo, and A. A. Boyarchuk, *Phys. Usp.* **55**, 115 (2012).
29. D. V. Bisikalo, A. G. Zhilkin, and A. A. Boyarchuk, *Gas-Dynamics of Binary Stars* (Fizmatlit, Moscow, 2013) [in Russian].
30. V. M. Lipunov, *Astrophysics of Neutron Stars* (Nauka, Moscow, 1987; Springer, Heidelberg, 1992).
31. P. Isakova, A. Zhilkin, and D. Bisikalo, *EPJ Web of Conferences*, **64**, id.03002 (2014).
32. D. A. Frank-Kamenetskii, *Lectures on Plasma Physics* (Atomizdat, Moscow, 1968) [in Russian].
33. F. F. Chen, *Introduction to Plasma Physics and Controlled Fusion* (Springer Science, New York, 1984; Moscow, Mir, 1987).
34. P.J. Meintjes, *Monthly. Not. Roy. Astron. Soc.* **352**, 416 (2004).
35. S.D. Drell, H.M. Foley, and M.A. Ruderman, *J. Geophys. Res.*, **70**, 3131 (1965).
36. A. V. Gurevich, A. L. Krylov, and E. N. Fedorov, *Sov. Phys. JETP* **48**, 1074 (1978).
37. R. R. Rafikov, A. V. Gurevich, and K. P. Zybin, *J. Exp. Theor. Phys.* **88**, 297 (1999).
38. L. D. Landau and E.M. Lifshits, *Course of Theoretical Physics, Vol. 8: Electrodynamics of Continuous Media* (Fizmatlit, Moscow, 2003; Pergamon, New York, 1984).
39. E. Parker, *Cosmical Magnetic Fields* (Clarendon, Oxford, 1979).
40. A. A. Ruzmaikin, D. D. Sokolov, and A.M. Shukurov, *Magnetic Fields of Galaxies* (Nauka, Moscow, 1988; Kluwer, Dordrecht, 1988).
41. D.P. Cox and E. Daltauit, *Astrophys. J.* **167**, 113 (1971).
42. A. Dalgarno and R.A. McCray, *ARA&A*, 375 (1972).
43. J.C. Raymond, D.P. Cox, and B.W. Smith, *Astrophys. J.* **204**, 290 (1976).
44. L. Spitzer, *Physical Processes in the Interstellar Medium* (Wiley, New York, 1978; Mir, Moscow, 1978).
45. D.V. Bisikalo, A. A. Boyarchuk, P. V. Kaigorodov, and O. A. Kuznetsov, *Astron. Rep.* **47**, 809 (2003).
46. A. G. Zhilkin and D. V. Bisikalo, *Astron. Rep.* **53**, 436 (2009).
47. A. G. Zhilkin, *Mat. Model.* **22**, No. 1, 110 (2010).
48. G.S. Bisnovatyi-Kogan and A.A. Ruzmaikin, *Astrophys. Space. Sci.* **42**, 401 (1976).
49. C.G. Campbell, *Magnetohydrodynamics in binary stars* (Dordrecht: Kluwer Acad. Publishers 1997).